Photoswitchable Magnetic Nanoparticles of Prussian Blue with Amphiphilic Azobenzene

Minori Taguchi,[†] Koji Yamada,[‡] Koji Suzuki,[‡] Osamu Sato,[§] and Yasuaki Einaga*[,†]

Department of Chemistry, Faculty of Science and Technology, Keio University, 3-14-1 Hiyoshi, Yokohama 223-8522, Japan, Department of Applied Chemistry, Faculty of Science and Technology, Keio University, 3-14-1 Hiyoshi, Yokohama 223-8522, Japan, and Institute for Materials and Engineering, Kyushu University, 6-1 Kasuga-koen, Kasuga 816-8580, Japan

Received May 18, 2005. Revised Manuscript Received June 24, 2005

A novel type of photocontrollable Prussian blue (PB) magnetic nanoparticle has been designed and prepared by using the reverse micelle technique. These magnetic nanoparticles possess a well-organized nanoscale structure. Reversible photoisomerization of azobenzene chromophores realized photoswitching of the magnetization. The photoisomerization of the composite materials was accompanied by a geometrically confined structural change within the reverse micelles, as reflected by changes in the dipole moment and the electrostatic field. As a result, the magnetization values could be switched reversibly by using alternating UV and visible light illumination.

Introduction

Photoswitchable materials are currently attracting great attention.[1,2] In particular, there has been great interest in designing novel compounds whose magnetic properties can be controlled by photoillumination.[3−7] Photocontrollable magnetic materials are important in the development of photonic devices, such as erasable optical memory media and optical switching components. However, the number of optically switchable molecular solids that have been reported is quite small, since an appropriate strategy for achieving photoinduced switching in a solid-state system has yet to be clarified.

To realize the reversible photoswitching of magnetization, we have previously presented a novel strategy of integrating magnetic materials into organized photoresponsive organic assemblies.[4,5] For example, in our previous work, we designed photocontrollable magnetic vesicles and LB films containing Prussian blue (PB) intercalated into an amphiphilic azobenzene moiety,[4] as well as photoresponsive amphiphilic photochromic compounds containing iron oxide particles.[5]

On the other hand, the properties of nanoscale particles have also recently been attracting a great deal of attention because of the ways in which they differ from the atomic, molecular, and bulk properties of those same materials.[8−12] Nanoparticles have uses in surface-chemical, photochemical, and other related fields; they are necessary for the preparation of some catalysts, and they can be used in magnetic materials, as constituents of paints, as semiconductors, as vehicles (polymer or otherwise) for in-vivo drug carriers, in molecular devices, and so on.[13−19] The field of magnetic materials has made use of variations in the magnetic properties of nano-

* To whom correspondence should be addressed. E-mail: einaga@chem.keio.ac.jp.
[†] Department of Chemistry, Keio University.
[‡] Department of Applied Chemistry, Keio University.
[§] Institute for Materials and Engineering, Kyushu University.

(1) (a) Irie, M. *Chem. Rev.* **2000**, *100*, 1685. (b) Alfimov, M. V.; Fedorova, O. A.; Gromov, S. P. *J. Photochem. Photobiol., A: Chem.* **2003**, *158*, 183.
(2) He, J.-A.; Mosurkal, R.; Samuelson, L. A.; Li, L.; Kumar, J. *Langmuir* **2003**, *19*, 2169.
(3) (a) Sato, O.; Iyoda, T.; Fujishima, A.; Hashimoto, K. *Science* **1996**, *272*, 704. (b) Sato, O.; Hayami, S.; Einaga, Y.; Gu, Z.-Z. *Bull. Chem. Soc. Jpn.* **2003**, *76*, 443. (c) Tokoro, H.; Ohkoshi, S.; Hashimoto, K. *Appl. Phys. Lett.* **2003**, *82*, 1245.
(4) (a) Einaga, Y.; Sato, O.; Iyoda, T.; Fujishima, A.; Hashimoto, K. *J. Am. Chem. Soc.* **1999**, *121*, 3745. (b) Einaga, Y.; Yamamoto, T.; Sugai, T.; Sato, O. *Chem. Mater.* **2002**, *14*, 4846. (c) Yamamoto, T.; Umemura, Y.; Sato, O.; Einaga, Y. *Chem. Mater.* **2004**, *16*, 1195.
(5) (a) Einaga, Y.; Taguchi, M.; Li, G.; Akitsu, T.; Gu, Z.-Z.; Sugai, T.; Sato, O. *Chem. Mater.* **2003**, *15*, 8. (b) Taguchi, M.; Li, G.; Gu, Z.-Z.; Sato, O.; Einaga, Y. *Chem. Mater.* **2003**, *15*, 4756. (c) Mikami, R.; Taguchi, M.; Yamada, K.; Suzuki, K.; Sato, O.; Einaga, Y. *Angew. Chem., Int. Ed.* **2004**, *43*, 6135.
(6) (a) Benard, S.; Leaustic, A.; Riviere, E.; Yu, P.; Clement, R. *Chem. Mater.* **2001**, *13*, 3709. (b) Nakatani, K.; Yu, P. *Adv. Mater.* **2001**, *13*, 1411.
(7) Li, G.; Akitsu, T.; Sato, O.; Einaga, Y. *J. Am. Chem. Soc.* **2003**, *125*, 12396.
(8) (a) Volokitin, Y.; Sinzig, J.; de Jongh, L. J.; Schmid, G.; Vargaftik, M. N.; Moiseev, I. I. *Nature* **1996**, *384*, 621. (b) Li, W.-H.; Yang, C. C.; Tsao, F. C.; Lee, K. C. *Phys. Rev. B* **2003**, *68*, 184507−1.
(9) Fendler, J. H. *Nanoparticles and Nanostructured Films*; Wiley-VCH: 1998.
(10) (a) Sun, S.; Zeng, H.; Robinson, D. B.; Raoux, S.; Rice, P. M.; Wang, S. X.; Li, G. *J. Am. Chem. Soc.* **2004**, *126*, 273. (b) Hyeon, T. *Chem. Commun.* **2003**, 927. (c) Han, M.; Vestal, C. R.; Zhang, Z. J. *J. Phys. Chem. B* **2004**, *108*, 583.
(11) (a) Vestal, C. R.; Zhang, Z. J. *J. Am. Chem. Soc.* **2003**, *125*, 9828. (b) Kataby, G.; Koltypin, Y.; Ulman, A.; Felner, I.; Gedanken, A. *Appl. Surf. Sci.* **2002**, *201*, 191. (c) Feldmann, C. *Adv. Funct. Mater.* **2003**, *13*, 101.
(12) (a) Quinlan, F. T.; Kuther, J.; Tremel, W.; Knoll, W.; Risbud, S.; Stroeve, P. *Langmuir* **2000**, *16*, 4049. (b) Martin, J. E.; Wilcoxon, J. P.; Odinek, J.; Provencio, P. *J. Phys. Chem. B* **2002**, *106*, 971. (c) Nickolov, Z. S.; Paruchuri, V.; Shah, D. O.; Miller, J. D. *Colloids Surf., A* **2004**, *232*, 93.
(13) (a) Fendler, J. H. *Chem. Rev.* **1987**, *87*, 877. (b) Fendler, J. H. *Membrane Mimetic Chemistry*; Wiley: New York, 1982. (c) Pileni, M. P. *Langmuir* **1997**, *13*, 3266.
(14) Israelachvili, J. N. *Intermolecular and Surface Forces*; Academic Press: London, 1989.

10.1021/cm051060c CCC: $30.25
Published on Web 07/29/2005

particles caused by effects such as single domains, superparamagnetism,[10] and surface interactions.[11] In particular, due to their large surface-to-volume ratio, the magnetic properties of nanoparticles are dominated by surface effects and particle−support interactions. They exhibit magnetic anisotropy constants that are 2 orders of magnitude larger than their bulk counterparts, with correspondingly enhanced coercivities.[10,11] Difficulties in the preparation of nanoparticles have been largely overcome by the use of water-in-oil (w/o) microemulsions.[13−14,16] The dispersed water pools that they contain act as microreactors in which a chemical reaction can be performed to generate the required product in the form of a colloidal nanodispersion. In this process, the size of the dispersant can be controlled such that the near-monodisperse state is favored and prolonged stability is ensured. The dispersed particles that are generated can be isolated by conventional physical−chemical means. In the recent literature, the preparations of metallic clusters,[12b,19] magnetic particles,[10a−b] complexes,[17,18] and metal oxides[10c,11] have also been reported. Details of the widespread research that has been conducted in this field (including the above-cited materials and other preparations, viz., ferrites, alloys, etc.) can be also found in recent reviews.[9,13]

PB and related cyanometalate-based coordination polymers offer a range of compounds that exhibit unique versatility.[3,20−21] PB is an important component in the study of molecular magnets because compounds with appropriate magnetic properties require further fabrication and processing if functional devices and materials are to be produced. Many attempts to synthesize PB analogue nanoparticles have recently emerged, making this a promising topic for nanomagnetic device applications.[17] Mann et al. first demonstrated this potential by confirming that hydrophobic PB nanoparticles with a uniform shape and size could be routinely prepared in a synthesis involving nanoscale water droplets formed in w/o microemulsions prepared from the anionic surfactant sodium bis(2-ethylhexyl) sulfosuccinate (AOT).[17a−b] Furthermore, Kitagawa et al. prepared highly dispersed PB nanoparticles that were controlled by organic polymers.[17c,d] They could control the size of the PB nanoparticles, and they studied the size dependence effect of the magnetic properties. However, photofunctional or photoresponsive nanoparticles of PB have never been developed. We have focused on the development of photoresponsive PB nanoparticles by using a reverse micelle technique in this work. Our strategy was to introduce a photoisomerizable azobenzene moiety to the PB reverse micelle as a surfactant. To form reverse micelles (w/o microemulsions) for PB, we have designed a new system containing both didodecyldimethylammonium bromide (DDAB) and {5-[4-((4-(dodecyloxy)phenyl)azo)phenoxy]hexyl}(2-hydroxyethyl)dimethylammonium bromide ($C_{12}AzoC_6N^+Br^-$) as appropriate surfactants. In our systems, it could be expected that positively charged these surfactants (DDAB and $C_{12}AzoC_6N^+Br^-$) interact with a negatively charged PB nanoparticles and colloids.[17d,i,j] The principle is based on the fact that the polymers can interact with growing a PB nucleus in the site-specific way.[17d] Moreover, another important point of the system is the homogeneous dilution of $C_{12}AzoC_6N^+Br^-$ in the coating DDAB in toluene solution. Although we have tried to dissolve azobenzene moieties in AOT w/o microemulsions system, we encountered difficulties in choosing an appropriate solvent. However, $C_{12}AzoC_6N^+Br^-$ could be dissolved perfectly in DDAB w/o microemulsions system and we could obtain photoresponsive PB nanoparticles.

DDAB

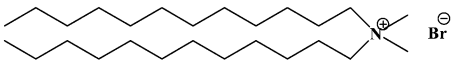

$C_{12}AzoC_6N^+Br^-$

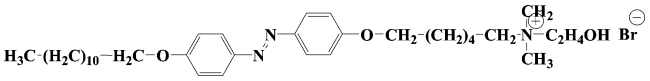

Experimental Section

Synthesis of Photofunctional PB Nanoparticles Using a Reverse Micelle Technique. Didodecyldimethylammonium bromide (DDAB) was purchased from Aldrich. $FeCl_2 \cdot 4H_2O$, $K_3[Fe(CN)_6]$, and toluene were purchased from Wako. Amphiphilic azobenzene, {5-[4-((4-(dodecyloxy)phenyl)azo)phenoxy]hexyl}(2-hydroxyethyl)dimethylammonium bromide ($C_{12}AzoC_6N^+Br^-$) was synthesized according to a procedure reported previously.[15−16b] Toluene and deionized water were bubbled with N_2 gas for 2 h before the experiment to remove oxygen. DDAB was first dissolved in toluene (0.1 M). The $FeCl_2 \cdot 4H_2O$ (15 μmol) and $C_{12}AzoC_6N^+Br^-$ (20 μmol) were then added to the DDAB solution. The mixture was sonicated until the entire solid disappeared and a clear yellow reverse-micelle solution was obtained. $K_3[Fe(CN)_6]$ was dissolved separately in deionized water (0.3 M). The $K_3[Fe(CN)_6]$ solution was slowly added to the reverse-micelle solution at room temperature to produce a DDAB w/o microemulsions at $w = 5$ with vigorous stirring. The microemulsions changed from a transparent yellow solution to a transparent blue solution at once, and no precipitate was observed for 1 week. Hereafter, this composite

(15) (a) Kunitake, T. *Angew. Chem., Int. Ed. Engl.* **1992**, *31*, 709. (b) Shimomura, M.; Ando, R.; Kunitake, T. *Ber. Bunsen-Ges. Phys. Chem.* **1983**, *87*, 1134. (c) Wei, W.-H.; Tomohiro, T.; Kodaka, M.; Okuno, H. *J. Org. Chem.* **2000**, *65*, 8979.
(16) (a) Kawai, T.; Hamada, K.; Kon-no, K. *Bull. Chem. Soc. Jpn.* **1993**, *66*, 2804. (b) Kaufman, S. *J. Colloid Interface Sci.* **1967**, *25*, 401.
(17) (a) Vaucher, S.; Li, M.; Mann, S. *Angew. Chem., Int. Ed.* **2000**, *39*, 1793. (b) Vaucher, S.; Fielden, J.; Li, M.; Dujardin, E.; Mann, S. *Nano Lett.* **2002**, *2*, 225. (c) Uemura, T.; Kitagawa, S. *J. Am. Chem. Soc.* **2003**, *125*, 7814. (d) Uemura, T.; Ohba, M.; Kitagawa, S. *Inorg. Chem.* **2004**, *43*, 7339. (e) Catala, L.; Gacoin, T.; Boilot, J.-P.; Rivière, É.; Paulsen, C.; Lhotel, E.; Mallah, T. *Adv. Mater.* **2003**, *15*, 826. (f) Moore, J. G.; Lochner, E. J.; Ramsey, C.; Dalal, N. S.; Stiegman, A. E. *Angew. Chem., Int. Ed.* **2003**, *42*, 2741. (g) Dominguez-Vera, J. M.; Colacio, E. *Inorg. Chem.* **2003**, *42*, 6983. (h) Yamada, M.; Arai, M.; Kurihara, M.; Sakamoto, M.; Miyake, M. *J. Am. Chem. Soc.* **2004**, *126*, 9482. (i) Hammond, P. T. *Adv. Mater.* **2004**, *16*, 1271. (j) DeLongchamp, D. M.; Hammond, P. T. *Adv. Funct. Mater.* **2004**, *14*, 224.
(18) Moulik, S. P.; De, G. C.; Panda, A. K.; Bhowmik, B. B.; Das, A. R. *Langmuir* **1999**, *15*, 8361.
(19) Lin, X. M.; Sorensen, C. M.; Klabunde, K. J.; Hajipanayis, G. C. *J. Mater. Res.* **1999**, *14*, 1542.
(20) (a) Robin, M. B. *Inorg. Chem.* **1962**, *1*, 337. (b) Ghosh, S. N. J. *Inorg. Nucl. Chem.* **1974**, *36*, 2465. (c) Ito, A.; Suenaga, M.; Ono, K. *J. Chem. Phys.* **1968**, *48*, 3597. (d) Herren, F.; Fischer, P.; Ludi, A.; Hälg, W. *Inorg. Chem.* **1980**, *19*, 956. (e) Buser, H. J.; Schwarzenbach, D.; Petter, W.; Ludi, A. *Inorg. Chem.* **1977**, *16*, 2704.
(21) (a) Ohkoshi, S.; Abe, Y.; Fujishima, A.; Hashimoto, K. *Phys. Rev. Lett.* **1999**, *82*, 1285. (b) Ferlay, S.; Mallah, T.; Ouahès, R.; Veillet, P.; Verdaguer, M. *Nature* **1995**, *378*, 701. (c) Holmes, H. S.; Girolami, G. S. *J. Am. Chem. Soc.* **1999**, *121*, 5593. (d) Buschmann, W. E.; Ensling, J.; Gütlich, P.; Miller, J. S. *Chem.*—Eur. J. **1999**, *5*, 3019.

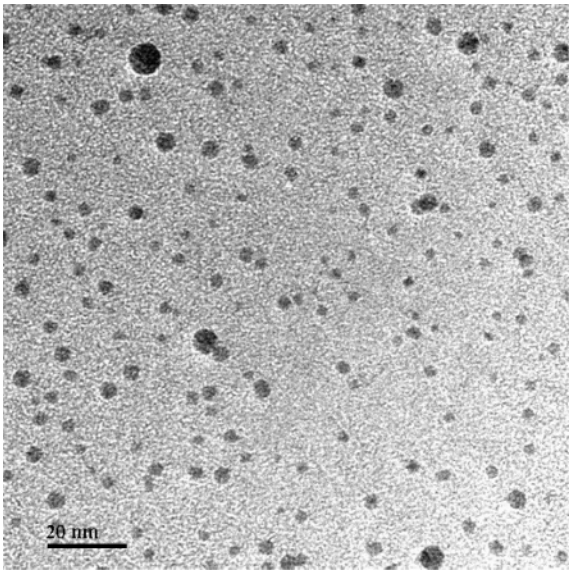

Figure 1. TEM image of **1**.

material is designated as **1**. Films of **1** were then prepared by casting the above solution onto glass substrates.

Physical Methods. UV−visible absorption spectra were recorded on a V-560 spectrophotometer (JASCO), and IR (Fourier transform infrared spectrometer) absorption spectra were recorded on a FT/IR-660 Plus (JASCO). A field emission transmission electron microscope (FE-TEM, TECNAI F20, Philips) was used to image the composite materials. The magnetic properties were investigated with a superconducting quantum interference device magnetometer (SQUID, MPMS-5S, Quantum Design). UV illumination (filtered light, $\lambda_{max} = 360$ nm, 10 mW/cm^2) was carried out using an Hg light source (Hypercure 200, Yamashita Denso). Visible illumination (filtered light, $\lambda_{max} = 450$ nm, 10 mW/cm^2) was carried out using a xenon light source (XFL-300, Yamashita Denso). X-ray diffraction (XRD) patterns were recorded on a Rigaku RINT RAD-RC with Cu Kα radiaton (Rigaku Co.).

Results and Discussion

Characterization of Composite Materials. Figure 1 shows a TEM image of a cast film of **1**. The TEM image indicates the presence of particles of **1** with almost homogeneous diameters (5 nm). To characterize the cast film of **1**, the XRD pattern and IR and UV−visible absorption spectra were monitored at room temperature. XRD analysis for **1** showed broad peaks at 16.7° (200) and 24.7° (220), which can be indexed as the PB cubic space group *Fm*3*m*.[20e] This indicates the presence of PB nanoparticles in **1**. The frequency of the CN stretching mode, ν(CN), of the PB nanoparticles in **1** was observed at 2073 cm^{-1}. This frequency was lower than that of bulk PB (2080 cm^{-1}), which corresponds to the CN stretching mode in the cyanometalate lattice.[20a,b] The UV−visible absorption spectra showed two intense peaks at 360 and 681 nm. The peak at 360 nm is ascribed to the $\pi-\pi^*$ transition of the trans-isomer of $C_{12}AzoC_6N^+Br^-$,[15a,b,23a] and the broad band at 681 nm is consistent with the intervalence charge transfer (IVCT) band (between $Fe^{III}(t_{2g}{}^3e_g{}^2)-CN-Fe^{II}(t_{2g}{}^6)$ and $Fe^{II}(t_{2g}{}^4e_g{}^2)-CN-Fe^{III}(t_{2g}{}^5)$) of PB nanoparticles in **1**. In general, the IVCT band of bulk PB was exhibited at ca. 700 nm.[20a] These peak shifts from the bulk PB in both the IR and UV−visible absorption spectra were due to the surface effect of nanoscale PB and were consistent with the results of AOT-reverse micelle PB.[17a]

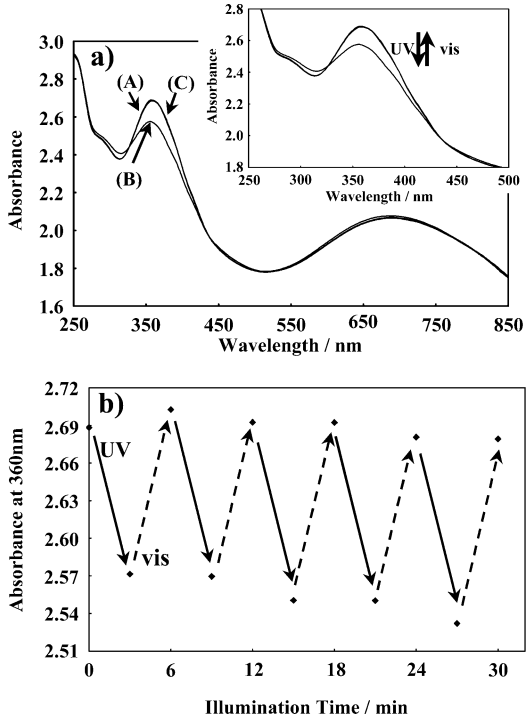

Figure 2. (a) Changes in the optical absorption spectra of **1** due to photoisomerization at room temperature. The initial trans state (A) was first illuminated with UV light for 3 min (B). Then, it was subsequently illuminated with visible light for 3 min (C). (b) Changes in absorbance at 360 nm by alternate illumination with UV and visible light. Each illumination was performed for 3 min. Reversible photoisomerization of **1** was demonstrated.

The photoisomerization of the $C_{12}AzoC_6N^+Br^-$ in **1** was monitored by UV−visible absorption spectroscopy at room temperature and 8 K. Typical UV−visible spectral changes due to photoisomerization at room temperature are shown in Figure 2a. Before illumination, **1** consisted solely of the trans-isomer of $C_{12}AzoC_6N^+Br^-$ (Figure 2a,A), because this is thermodynamically more stable than the cis-isomer.[23a] Illumination of the trans-isomer with UV light converted it to the cis-isomer. The peak at 360 nm decreased, while a weak peak appeared at ca. 470 nm (Figure 2a,B). The 470 nm peak is ascribed to the n$-\pi^*$ transition of the cis-isomer. After subsequent illumination with visible light, the reverse process (Figure 2a,C), i.e., the cis-to-trans isomerization, proceeded. Therefore, the spectra obtained before and after the complete UV−visible illumination cycle were identical (Figure 2b). Similar results were also obtained at 8 K (not shown). In general, it is known that the solid-state reaction (trans-to-cis photoisomerization) is greatly inhibited due to the close-packing of the chromophores. This is because the photoisomerization of the azobenzene derivatives (particu-

(22) (a) Brown, G. H. *Photochromism*; Wiley: New York, 1971. (b) Tachibana, H.; Yamanaka, Y.; Matsumoto, M. *J. Mater. Chem.* **2002**, *12*, 938.

(23) (a) Diau, E. W.-G. *J. Phys. Chem.* **2004**, *108*, 950. (b) Hartley, G. S.; Le Fèvre, R. J. W. *J. Chem. Soc.* **1939**, 531. (c) Higuchi, M.; Minoura, N.; Kinoshita, T. *Macromolecules* **1995**, *28*, 4981. (d) Yu, Y.; Nakano, M.; Ikeda, T. *Nature* **2003**, *425*, 145.

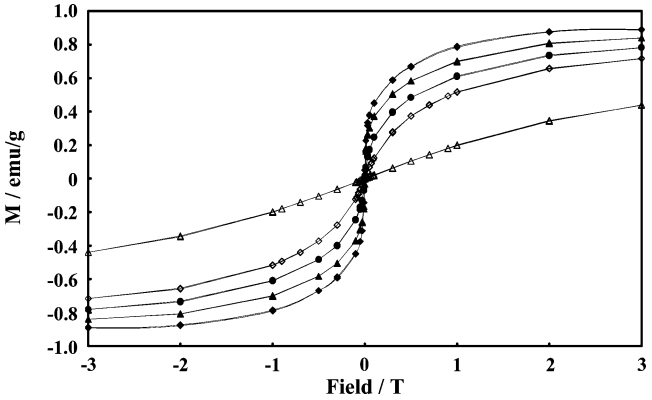

Figure 3. Magnetization versus applied magnetic field for **1** at (◆) 2 K, (▲) 3 K, (●) 4 K, (◇) 5 K, and (△) 10 K.

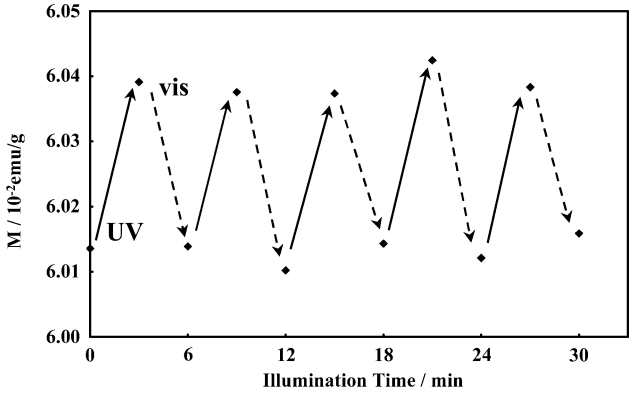

Figure 4. Changes in the magnetization of **1** induced by UV and visible light illumination at 2 K with an external magnetic field of 1 mT.

larly the trans-to-cis isomerization reaction) is accompanied by an increase in molecular volume.[23c] Normally, the photoisomerization of azobenzene derivatives in the solid state can only be observed in special environments, such as in bilayer membranes,[4a−b] LB films,[4c] liquid crystal matrixes,[4d] etc. However, in the present system, photoisomerization of the $C_{12}AzoC_6N^+Br^-$ was observed in the reversed micelles, even on solid substrates.

Magnetic Properties of Photofunctional Materials. The magnetic properties of **1** cast onto a glass substrate were measured by SQUID. The magnetization curves were measured at several temperatures (2, 3, 4, 5, 10 K), and the results are shown in Figure 3. **1** exhibited superparamagnetic behavior, as indicated by the zero coercivity and remanence on the magnetization curve. Furthermore, as the temperature was increased, the magnetization curve exhibited linear paramagnetic behavior. Because of their nanoscale level, the anisotropy energy barriers for magnetic nanoparticles are smaller than for the bulk material. Therefore, thermal energy can overcome the anisotropy barrier at high temperature, allowing a coherent rotation of the atomic moments of a particle. Each particle then behaves like a giant atom with a large moment, a phenomenon known as superparamagnetism.[10−11,19] Bulk PB exhibits ferromagnetic behavior below a Curie point T_C of 5.5 K.[20a,c−d] It is known that the magnetic properties of PB are due to effective magnetic moments corresponding to high-spin Fe^{III} and diamagnetic low-spin Fe^{II}. Ferromagnetism obviously requires long-range ordering of the spins of the Fe^{III} ions. The two shortest Fe^{III}−Fe^{III} interatomic distances in the structure of PB are 7.2 Å through space and 10.2 Å along the sequence Fe^{III}−NC−Fe^{II}−CN−Fe^{III}. A superexchange mechanism along this sequence is assumed to be the most plausible mechanism, with a mixed-valence interaction leading to a small spin transfer from Fe^{III} to Fe^{II}.[20d]

The effects of the illumination of **1** with light at 2 K under an external magnetic field of 1 mT are shown in Figure 4. During illumination with UV light for 3 min, the magnetization value increased from 6.01×10^{-2} to 6.04×10^{-2} emu/g. Even after the illumination was stopped, this enhanced magnetization was maintained for at least 2 h. Then we illuminated the sample with visible light for a further 3 min. The magnetization value decreased to 6.01×10^{-2} emu/g. After this process, the UV-light-induced increase and visible-light-induced decrease of the magnetization were repeated several times. These magnetization changes are consistent with the UV−visible absorption spectral changes (Figure 2) and can be explained in the same fashion. To confirm the effect of the azobenzene moiety, PB nanoparticles that were only encapsulated with DDAB were prepared (without $C_{12}AzoC_6N^+Br^-$), and these were designated as **2**. A TEM image of **2** also showed the presence of global PB nanoparticles with almost homogeneous diameters (5 nm), while magnetic measurements of **2** exhibited almost the same properties as **1** (not shown). However, when **2** was illuminated with either UV or visible light, no changes were observed in the total magnetization. This result suggests that the $C_{12}AzoC_6N^+Br^-$ in **1** plays an important role in the photocontrol of the magnetization. Furthermore, photocontrollable magnetization could not be observed in the case where only surfactants (DDAB and $C_{12}AzoC_6N^+Br^-$) and bulk PB were present.

Electrostatic Interaction between PB Nanoparticles and $C_{12}AzoC_6N^+Br^-$. We have focused on the interaction between PB nanoparticles and $C_{12}AzoC_6N^+Br^-$ as the mechanism for photocontrollable magnetization. The absorption maximum, λ_{max} (the IVCT band from Fe^{II} to Fe^{III} of the PB nanoparticles), for composite material **1** was observed at 681 nm.

As mentioned before, the blue shift is due to the size effect of the PB. That is, the existing electrostatic fields heighten the Coulombic energy required to transfer electrons from hexacyanoferrate (Fe^{II}) ions to the surface Fe^{III} species. Figure 5 shows the changes in value of λ_{max} before and after the alternating photoillumination. After UV illumination, the λ_{max} peak was red-shifted. That is, the photoisomerization of the azobenzene moiety from trans to cis lowered the Coulombic energy. Then, after visible light illumination, the λ_{max} peak was blue-shifted; i.e., it heightened again. This reversible change was repeated several times by alternate illumination with UV and visible light. Similar results were also obtained at 8 K (not shown). By analogy with our previous system, it is proposed that photoisomerization of the $C_{12}AzoC_6N^+Br^-$ was accompanied by a geometrically confined structural change,[23a] as reflected by changes in the dipole moment[23b] and the electrostatic field. This reversible change is almost consistent with the changes in the magnetization (Figure 4). The trends of the UV-light-induced red-shift and the visible-

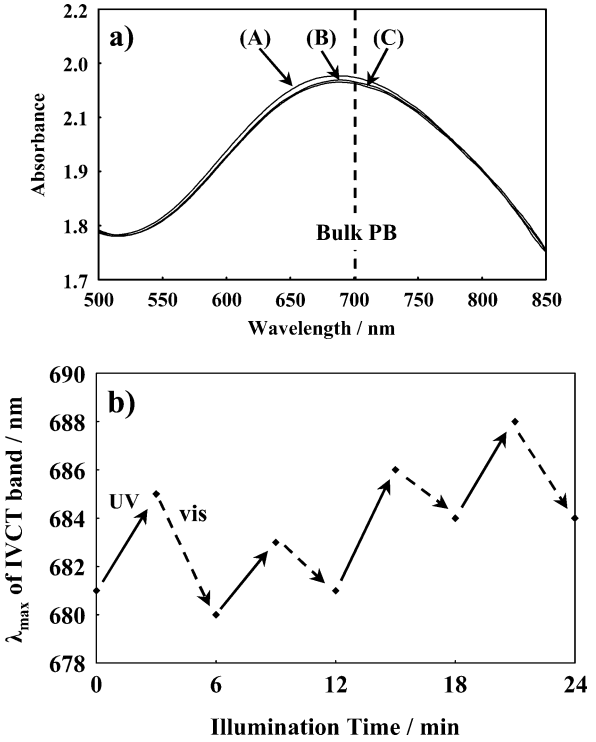

Figure 5. Changes in the absorption spectra for **1** in the region of the IVCT band from Fe^{II} to Fe^{III} in the PB nanoparticles by alternate UV and visible light illumination. The initial trans state (A) was first illuminated with UV light for 3 min (B). Then, it was subsequently illuminated with visible light for 3 min (C). (b) Changes in the IVCT band from Fe^{II} to Fe^{III} in PB nanoparticles induced by alternate UV and visible light illumination. Each illumination was performed for 3 min.

light-induced blue-shift of the IVCT band of PB in our previous system[4] were consistent with the results of the present system. However, the UV-induced increase and the visible light-induced decreasing trend in the present system were the opposite of our observation for our previous system. This is because of the difference of the existing electrostatic field, which affects the spin polarization on the Fe^{II-LS}. Basically, in this work, the electrons on the synthesized PB that occupy the t_{2g} orbital on the $Fe^{II-LS}(t_{2g}^6e_g^0)$ are partly delocalized onto the neighboring $Fe^{III-HS}(t_{2g}^3e_g^2)$, and we could modulate the spin polarization on the Fe^{II-LS} from that of the bulk state by introducing a surfactant, etc. The magnetic value is highest when the electrostatic field around the Fe^{II-LS} is the same as the bulk PB (IVCT band for $Fe^{II}-CN-Fe^{III}$ = 700 nm). That is, the magnetization value increases when the IVCT band approaches 700 nm, and vice versa.

Detailed Mechanism of Photoswitchable Magnetization. It has been suggested that photoinduced changes in the electrostatic field around the PB nanoparticles can affect the magnetization. Examples from our previous work could also be explained by similar interactions.[4] Changes in the dipole moments induced by the photoisomerization of the $C_{12}AzoC_6N^+Br^-$-induced magnetic fields and moments in the PB nanoparticles. Figure 6 shows a schematic illustration of the photoinduced switching of the magnetization.

Sato et al. described another typical example of changes in magnetic properties that were observed for PB that was prepared by using electrochemical control.[3b] When the

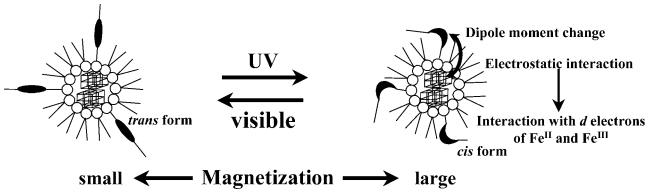

Figure 6. Schematic illustration of photoswitching of the magnetization of **1**. Changes are shown in the dipole moments induced by the photoisomerization of $C_{12}AzoC_6N^+Br^-$-induced electrostatic interactions between the changed dipole moment of $C_{12}AzoC_6N^+Br^-$ and the magnetic species of the PB nanoparticles. As a result, the magnetization was affected.

electronic state of the $Fe^{II}-CN-Fe^{III}$ (IVCT) in PB is changed, the magnetic properties also change progressively. This modification of the magnetic properties arises mainly from a change in the degree of valence delocalization. The electrons in the PB that formerly occupied the t_{2g} orbital on the $Fe^{II-LS}(t_{2g}^6e_g^0)$ are partly delocalized onto the neighboring $Fe^{III-HS}(t_{2g}^3e_g^2)$. Since the t_{2g} and e_g orbitals of the Fe^{III-HS} are both exactly half-occupied, it is energetically favorable to delocalize only one type of spin (α or β spin) from the Fe^{II-LS} to the Fe^{III-HS} due to the Coulomb and exchange repulsion terms. The spin polarization on the Fe^{II-LS} induces a magnetic correlation between the Fe^{III-HS}, leading to magnetic ordering at 4.2 K. On the other hand, after reduction, the electronic state is converted to $Fe^{II-LS}(t_{2g}^6e_g^0)-CN-Fe^{III-HS}(t_{2g}^4e_g^2)$ and hence partial delocalization of the electrons from the Fe^{II-LS} to the Fe^{III-HS} (or vice versa) is prevented due to a large Coulomb repulsion. Thus, the spin polarization on the Fe^{II-LS} almost disappears, which results in the reduction of the magnetic interaction between the Fe^{II-HS} through the Fe^{III-LS}. As a consequence, the compound shows ferromagnetic-to-paramagnetic interconversion by electrochemical reduction. Furthermore, when the PB is oxidized to $Fe^{III}_4[Fe^{III}(CN)_6]_3$, then T_C progressively increases. This is consistent with the fact that the diamagnetic component, $Fe^{II-LS}(t_{2g}^6e_g^0)$, is oxidized to $Fe^{III-LS}(t_{2g}^5e_g^0)$ with one unpaired electron in the t_{2g} orbital.

Furthermore, Zhang et al. studied the effects of surface coordination chemistry on the magnetic properties of $MnFe_2O_4$ nanoparticles.[11a] They observed that the coercivity of the magnetic nanoparticles decreased upon coordination of the ligands on the nanoparticle surfaces, whereas the saturation magnetization increased. They concluded that the change in the magnetic properties of the nanoparticle surfaces and the correlations suggest a decrease in the spin−orbital coupling and surface anisotropy of the magnetic nanoparticles due to surface coordination. Gedanken et al. also studied the magnetic properties (especially the blocking temperature, T_B) of iron nanoparticles coated with various surfactants.[11b] They observed large variations in blocking temperature for various functional groups bonded to the iron nanoparticles. For example, the magnetization values for alcohols and carboxylic acids were different from those for sulfonic acid. They also discussed how these differences could be explained, not only by variations in particle size but also through the effects of having the functional group bonded to an iron atom on the d electrons and therefore causing a large splitting of the doubly and triply degenerate d levels. This affects the spin state and the magnetization values. Anyhow, this suggests

that exchange interactions between the spins of the iron affect the magnetization.

The above discussions also suggest that photoinduced changes in the electrostatic field around the PB nanoparticles affect the magnetization. Photoswitchable magnetic films (PB intercalated in Langmuir−Blodgett films consisting of an amphiphilic azobenzene and a clay mineral), which was one of our previous photofunctional systems,[4c] supplied data that support these mechanisms. The IVCT band between the Fe^{II} and the Fe^{III} in the PB nanoparticles was changed reversibly by alternating UV and visible light illumination, accompanied by photoisomerization of the azobenzene chromophores that lead to changes in the Coulombic energy (which is necessary to transfer an electron), and this might affect the superexchange interaction between the spins in the PB magnet.

The small photoinduced change of the magnetization is consistent with the small photoisomerization. Furthermore, the present system using reverse micelle technique has a disadvantage point for large control of the magnetization, because there is no direct chemical bonding between $C_{12}AzoC_6N^+Br^-$ and PB nanoparticles. We have already reported the azobenzene moiety modified iron oxide nanoparticles, which showed the large (ca. 10%) photocontrol of magnetization.[5c] This is because the azobenzene moieties coordinate with iron atoms on the surface of γ-Fe_2O_3 nanoparticles directly. That is, small electrostatic interaction between $C_{12}AzoC_6N^+Br^-$ and PB nanoparticles through binding water affected the magnetization in the present system, similar to our first example.[4a]

Conclusion

Photocontrollable PB nanoparticles have been developed in the solid state. As a result, we succeeded in introducing photofunctionality to molecule-based magnetic materials on a nanoscale level. This work will yield much valuable information, bringing not only new perspectives into photofunctional materials derived from a combination of photofunctional organic materials and inorganic magnetic materials but also future applications of nanomagnetic materials, which are currently attracting growing interest in ultrahigh-density magnetic recording systems.

Acknowledgment. This work was supported by a Grant-in-Aid for Scientific Research on Priority Areas (417) and the 21st Century COE program "KEIO Life Conjugate Chemistry" from the Ministry of Education, Culture, Sports, Science, and Technology (MEXT) of the Japanese Government.

CM051060C